Short Notes

Improved Relative Locations of Clustered Earthquakes Using Constrained Multiple Event Location

by Michael Fehler, W. Scott Phillips, Leigh House, R. H. Jones, Richard Aster, and Charlotte Rowe

Abstract   A new method for improving relative locations of clustered earthquakes is presented and applied to a suite of microearthquakes induced by hydraulic fracturing. The method is based on the assumption that clustering of earthquake hypocenters is obscured by the uncorrelated scatter of individual hypocenters. The method is implemented as an additional constraint in a Joint Hypocenter Determination (JHD) scheme. The method shifts event hypocenters toward the center of mass of the events within some volume surrounding the event location if the RMS misfit between predicted and measured arrival times does not increase significantly. The method uses the same basic assumption of Jones and Stewart (1997), which is that there is greater clustering in actual earthquake locations than there is in locations determined using conventional techniques. Our method differs in that it is implemented as part of the JHD process so it operates on raw travel-time data rather than on derived hypocenters. The method produces hypocenters from a demonstration field dataset that are similar to those obtained by Phillips *et al.* (1997), from time-consuming precise manual repicking of relative arrival times of events. The clustering constraint can easily be incorporated as an additional constraint in earthquake location/velocity tomography codes and may lead to improved velocity structure determination and earthquake location pattern identification and interpretation.

Introduction

Since seismologists began locating earthquakes using travel times from seismic networks, they have attempted to relate patterns of locations to geological and tectonic structures. Although this is usually done by visual inspection of earthquake location maps, new analytical methods have been introduced to help identify structures within seismic zones. Michelini and Bolt (1986) introduced a principal components method to identify clusters of seismic events in space and time. In this method, one forms a covariance matrix from the earthquake location coordinates and computes the principal axes of the matrix, which are the axes of an ellipsoid that encompasses the events. Fehler *et al.* (1987) developed the Three Point Method, which is a statistical method to identify planes in earthquake zones. These planes are interpreted to be fracture planes and their orientations agree with failure planes expected from in situ stress fields (Fehler, 1989). This method was used to study aftershocks of the 1983 Coalinga earthquake (Fehler and Johnson, 1989). It has also been implemented in a manner to help to identify the plane of slip in a fault-plane solution (Fehler, 1990). Amorese *et al.* (1999) recently proposed a point-pattern

method for identifying patterns in sparse hypocenter location datasets. Relative locations of events that have similar waveforms have been determined by taking advantage of the similarity of waveforms to pick precise relative arrival times for the events (Poupinet *et al.,* 1984; Ito, 1985; Fremont and Malone, 1987; Moriya *et al.,* 1994; Nadeau *et al.,* 1995; Dodge *et al.,* 1996; Gillard *et al.,* 1996; Phillips *et al.,* 1997; Shearer, 1997, 1998; Rubin *et al.,* 1999) and to constrain Green Function variability (Aster *et al.,* 1990; Haase *et al.,* 1995). The maps of relative locations determined in many of these studies show significant structures that could not be found in the maps made from locations determined using conventional location approaches.

Jones and Stewart (1997) introduced a method they refer to as "collapsing", in which event hypocenters are moved within a confidence interval in a direction toward the center of mass of the events within the interval. The confidence interval they use is an error ellipsoid having dimensions equal to four standard deviations of the location uncertainty, which corresponds to a 99.86% confidence. The argument for shifting event locations is that locations could reside any-

where within the error ellipsoid with little change in the RMS misfit to the arrival-time data. Jones and Stewart (1997) demonstrate that structures are clearly delineated within a seismogenic ring-fracture zone around Rabaul Volcano, Papua New Guinea, after the events have been collapsed.

In this article we demonstrate a slightly different approach for collapsing event hypocenters that can be incorporated into the location-inversion algorithm itself. We call our method Joint Hypocenter Determination (JHD)-collapsing. We find that the method produces only a slight change in the misfit of the arrival times but that the resulting hypocenters are significantly more clustered than those found using JHD alone. The alignments of events found by Phillips *et al.* (1997) from visual cross-correlation and manual re-picking of relative arrival times of a group of events that have similar waveforms can be recovered using the original arrival-time picks and the new analysis method. The agreement between the JHD-collapsing results and those of Phillips *et al.* (1997) demonstrates the ability of the JHD-collapsing method to find significant structures within a zone of seismicity that cannot be found in locations determined using traditional JHD alone.

Approach

In the conventional JHD approach, arrival-time data are inverted to find the event locations, event origin times, and station corrections that minimize

$$\sum_{ij} R_{ij}^2 = \sum_{ij} \left\{ \left(\frac{t_{ij}^{pm} - t_{ij}^{pe}}{\sigma_{ij}^p} \right)^2 + \left(\frac{t_{ij}^{sm} - t_{ij}^{se}}{\sigma_{ij}^s} \right)^2 \right\} \quad (1)$$

where t_{ij}^{pm} is the measured P time at station i for event j, t_{ij}^{pe} is the predicted time for the same station-event pair given the estimated earthquake location and origin time, and t_{ij}^{sm}, t_{ij}^{se} are the corresponding times for S waves. Weighting of arrival times can be accomplished by choosing σ_{ij}^p and σ_{ij}^s. The minimization of equation (1) is done using an iterative scheme in which a set of equations are set up for each earthquake that relate the change in earthquake location, change in earthquake origin time, and change in station correction to the difference in observed and predicted arrival times at each station for the earthquake location, origin time, and station corrections calculated from the previous iteration. For a given earthquake having p travel-time observations, a total of p equations of the form $\delta t_i = h_{iq} \, \delta x_q$ are used. Following Menke (1984, pp 201–205) δt_i is the difference between observed and predicted travel time for the ith observed travel time for the event; δx_q is the solution vector composed of the changes in the earthquake location, origin time, and station corrections for the given iteration; and h_{iq} is a matrix of partial derivatives relating changes in travel-time residuals to earthquake location parameters and station corrections. For a suite of events, we combine the equations for all events and solve them in a manner to minimize the sum squared of travel-time residuals. In the JHD-

collapsing approach, we choose a sphere of radius r around each event and find the center of mass of all events that lie within the sphere (shown in Figure 1). We then modify the function that is minimized to be

$$\sum_{ij} R_{ij}^2 + \lambda \sum_j C_j^2 = \sum_{ij} \left\{ \left(\frac{t_{ij}^{pm} - t_{ij}^{pe}}{\sigma_{ij}^p} \right)^2 \right.$$
$$\left. + \left(\frac{t_{ij}^{sm} - t_{ij}^{se}}{\sigma_{ij}^s} \right)^2 \right\} + \lambda \sum_j \sum_k \{ (x_{jk} - x_{jk}^{cm})^2 \} \quad (2)$$

where $k = 1, 3$ (x_{j1}, x_{j2}, x_{j3}) is the location of event j, ($x_{j1}^{cm}, x_{j2}^{cm}, x_{j3}^{cm}$) is the center of mass of the events surrounding event j, and C_j is the distance between event j and the center of mass for that event. The first term in equation (2) is the residual term (defined in equation 1), and we refer to the second term as the collapse constraint term. We incorporate JHD-collapsing into the iterative solution process as a constraint by adding three equations for each event to the set of equations to be solved for that event in the iterative location scheme (see Menke, 1984, pp 55–57). The three equations express the constraint in a form $S_{jk} = T_{km} (dx_{jm})$, $k = 1,3$, $m = 1,3$ where dx_{jm} is the change in the mth component of the location of event j, $S_{jk} = \sqrt{\lambda} (x_{jk} - x_{jk}^{cm})$, and $T_{km} = \sqrt{\lambda} \delta_{km}$ where δ_{km} is the Kronecker delta. The solution of the set of equations then proceeds as in JHD. The collapse constraint introduces two free parameters; the radius of the sphere, r, and the multiplier, λ. In practice, the radius of the sphere may be based on the estimated uncertainties in the locations of the events and the requirement that there be some minimum number of events within the
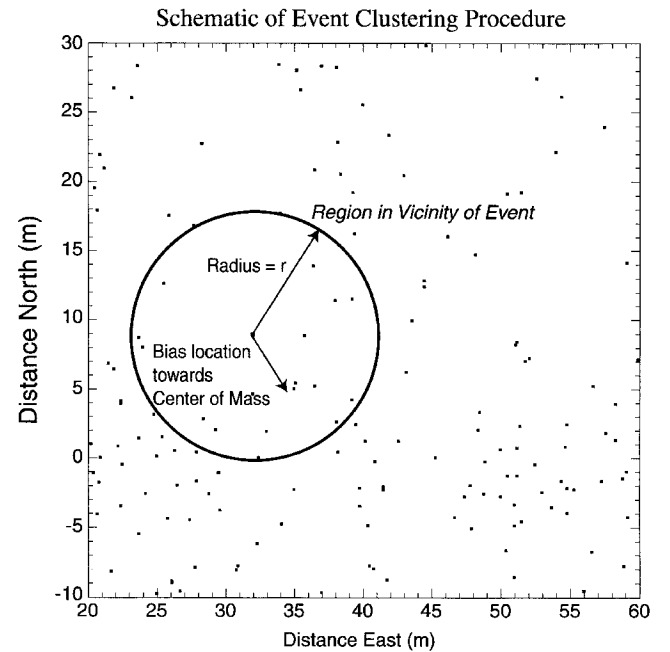

Figure 1.   Schematic of constraint applied to event location in analysis procedure. Each event location is biased toward the center of mass of the other events in its vicinity.

sphere surrounding most events. The radius of the sphere does not enter explicitly into the location scheme. The value of λ may then be chosen so that the collapse constraint term has about the same magnitude as the residual term in equation (2). We choose these two parameters using test calculations with synthetic data.

Following Jones and Stewart (1997), we could replace the sphere with an error ellipsoid determined from the location procedure. For simplicity, we have chosen not to do this. The error ellipsoid for a given earthquake location indicates how much the event location may be shifted without significantly changing the travel-time residuals for the event. If an error ellipsoid is nonspherical, the event may be moved more along the direction of the major axis of the error ellipsoid than in other directions for the same relative change in travel-time residuals. In our procedure, we trade off travel-time residuals and the shifting of the event location toward the center of mass of the events within a sphere surrounding the event. If a shift in one direction significantly increases the travel-time residuals, the event is not allowed to move in that direction. Shifting is thus implicitly controlled by the dimensions and shape of the error ellipsoid although an ellipsoid is not explicitly used in the calculation of equation (2).

We implemented the constraint given in equation (2) into the JHD code described by Block *et al.* (1994). This method is a procedure for simultaneously locating earthquakes and finding station corrections that provide a best fit to the arrival-time data for all events. We used a homogeneous velocity model in our testing described subsequently. Station corrections and improved locations are iteratively determined using the JHD collapsing approach with the station corrections and locations determined from the previous iteration. The center of mass of events surrounding each event is recalculated during each iteration using the location distribution from the previous iteration.

Figure 2 shows an example of applying the JHD-collapsing method to a synthetic data set. For this test, 3000 events were distributed within a 200 m by 200 m by 200 m volume. The events were chosen so that 400 of them fell along an east-west trending plane, 400 along a north-south trending plane, 200 along a NE-SW trending plane, and the remaining 2000 were scattered uniformly within the region. Both *P* and *S* travel times were calculated to four stations for all events and noise having zero mean and 0.7 ms standard deviation was added to the travel times. Station locations are taken as the four located at the Fenton Hill Hot Dry Rock Geothermal Energy site in New Mexico (Block *et al.,* 1994). The four stations are located at distances of about 500 m to 3 km from the center of the seismic zone. One station is located directly above the zone and the remaining three stations surround the zone of seismicity. *P*- and *S*-wave velocities were 5.92 km/sec and 3.5 km/sec, respectively. Figure 2a shows event locations used to generate the traveltimes. Figure 2b shows locations determined using conventional JHD on the noisy travel-time data. The three event planes can be seen but are not clear. Figure 2c shows the locations determined using the JHD-collapsing approach
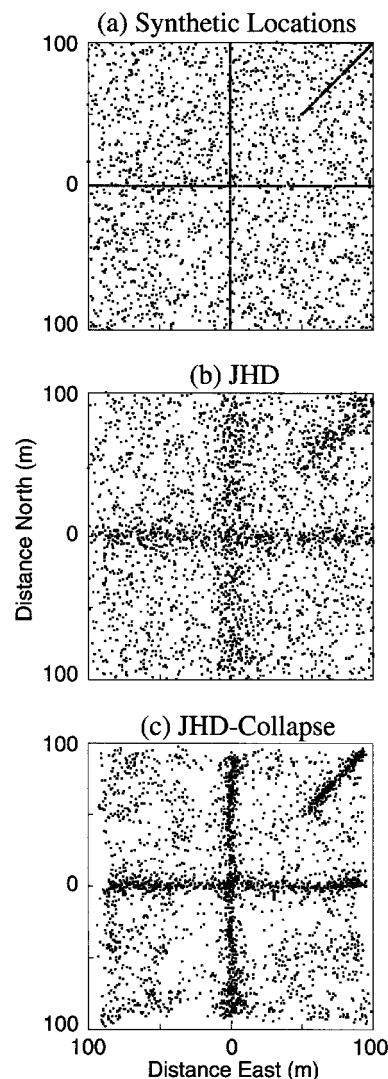

Figure 2. Test of the collapsing method on synthetic data. Locations of events are projected onto a horizontal plane. (a) Original locations, (b) locations found using JHD with noisy data, (c) locations found using JHD-collapsing method with noisy data.

with $\lambda = 1 \ \text{sec}^2/\text{m}^2$ and $r = 30$ m. These values are appropriate for the type of station geometry and type of data collected at the Fenton Hill site. The location distribution determined using the JHD-collapsing approach shows the alignments of events along the three planes more clearly than does the ordinary JHD approach, yet the density of events in the zone surrounding the three planes is lower than in the original dataset (Figure 2a). This reduction arises from the shifting of events located near the planes in a direction toward the planes. Interpretation of location patterns produced by the JHD-collapsing should therefore take account of the tendency of the method to prefer collapsed structures.

Application

To test the collapsing approach with real data, we chose data from the Fenton Hill Hot Dry Rock Geothermal Energy

project in northern New Mexico USA. Locations of these events and stations have been discussed by House (1987), Fehler *et al.* (1987), Fehler (1989), Block *et al.* (1994), and Fehler *et al.* (1998). We investigate a dataset consisting of approximately 9900 of the best located events. Arrival times from *P* and *S* waves recorded at four borehole seismometers were used to locate these events. Arrival times were manually picked from waveforms for each event. The same homogeneous velocity model used in the synthetic test above was used to analyze these data. Arrival times of *P* and *S* waves at each station were weighted in a manner identical to that of Block *et al.* (1994). Figure 3 shows North-South vertical cross-sections of three different sets of event loca-

tions. Figure 3a shows the initial locations determined using a single-event location technique. Figure 3b shows the locations determined using traditional JHD. Figure 3c shows the locations found using the JHD-collapsing method. Locations shown in Figure 3c were calculated using $\lambda = 1$ sec^2/m^2 and $r = 30$ m. The location pattern in Figure 3c shows more structure and event clustering than can be seen in Figure 3a or 3b. Table 1 gives the values of the average traveltime residuals for both *P* and *S* waves for locations determined using the three procedures. Travel-time residuals from JHD-collapsing are substantially lower than those for the single-event procedure, but are slightly greater than those from conventional JHD. The value of the center of mass
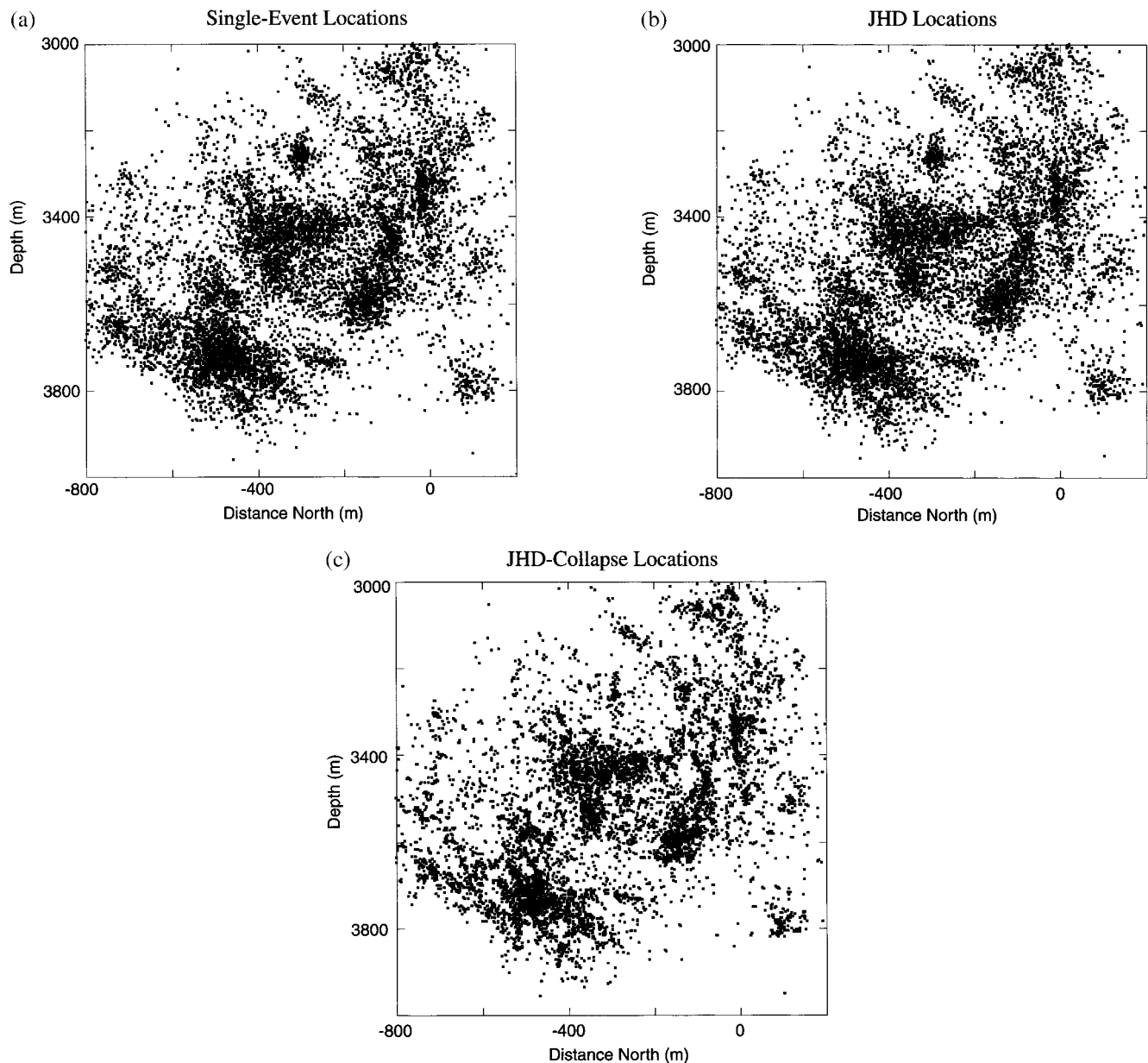

Figure 3.   North-South vertical cross sections through the locations of induced seismic events at Fenton Hill determined using (a) single-event location technique, (b) JHD, (c) JHD-collapsing.

Table 1
Arrival-Time Residuals (msec) after Locating Events.

	P Waves	*S* Waves
Single Event Location Technique	2.12	2.46
JHD	1.04	1.92
JHD-Collapsing	1.11	2.06

constraint, the right hand term in equation (2), averages 1.95 sec^2/m^2 for the first iteration of the JHD-collapsing procedure and 1.16 sec^2/m^2 for the final iteration. The changes in hypocenters are extremely small (8-m average), and the accompanying changes in RMS residual for *P* and *S* waves are also small. However, the difference in the pattern of earthquake locations is substantial.

To investigate the structure within the seismic zone in more detail, Figure 4 shows map views of 3238 locations shown in Figure 3 that fall within a cube of 400 m on a side and in the depth range 3500–3900 m. The region shown was identified by Phillips *et al.* (1997) as having a number of clusters, each generating microearthquakes with similar waveforms. Figure 4a shows the single-event locations for all the events. Figure 4b shows the locations found with conventional JHD. Conventional JHD generally provides better relative locations, and although no distinct features can be seen, the earthquake distribution in Figure 4b shows more clustering of events than is shown in Figure 4a. Figure 4c shows the locations found using JHD-collapsing, which shows significantly more clustering than do the single event or conventional JHD locations. Phillips *et al.* (1997) manually picked precise relative arrival times of the events having similar waveforms. They relocated these events using a master-event technique and found that they fell along planar features. Figure 4d shows these relocations that contain a number of planar structures, two of which dip steeply and can be seen in this view. These planar features were interpreted to be individual slipping joint surfaces that were activated by the hydraulic fracturing. Comparing Figures 4c with 4d, we see that the JHD-collapsing technique has recovered
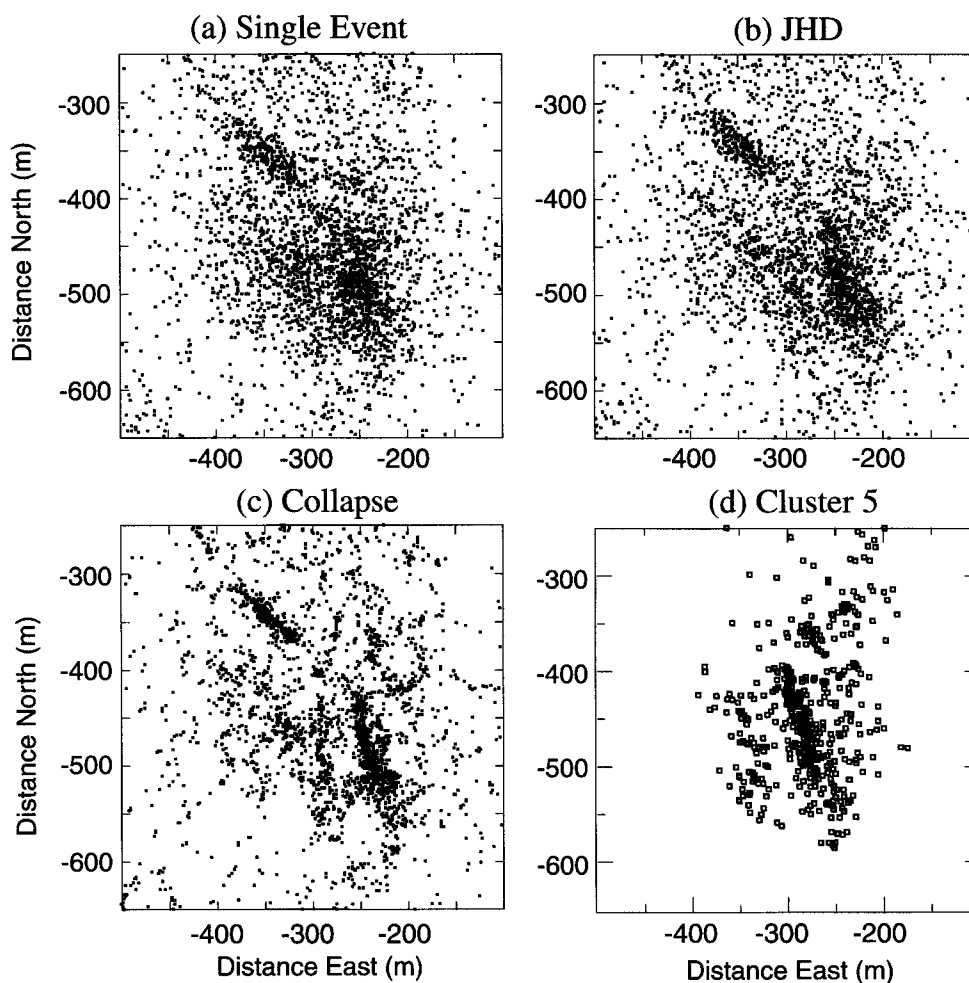

Figure 4.   Locations of Fenton Hill events within a cube having dimensions of 400 m on a side. (a) locations from single event location method. (b) JHD locations (c) locations from JHD-collapsing method (d) locations found by Phillips *et al.* (1997) using relative arrival time picks for the subset of events exhibiting similar waveforms.

many of the planar features found using precise relative picking of events. Additional features are apparent in the JHD-collapsing locations, which were not included in the data set analyzed manually by Phillips *et al.* (1997). The difference in absolute event locations found by the JHD-collapsing approach and the precise manual picking approach results from the difference in station corrections used by the two methods. Phillips *et al.* (1997) based station corrections on a master event, whereas the JHD-collapsing procedure calculates station corrections.

Conclusions

We presented a method, which we call JHD-collapsing, for obtaining better relative locations of earthquakes within a zone of seismicity if it can be assumed that seismogenic regions are dominated by spatial clustering of events. The results of using the JHD-collapsing method are consistent with those found using a much more laborious method, namely manual repicking of relative arrival times for events having similar waveforms. The new method has the capability of finding features in a seismic zone that may not be found by manual analysis of event clusters because more events can be analyzed using the new method. Since the method involves the introduction of a single additional collapsing-constraint on the traditional JHD, it is in a form that can be conveniently used to find seismogenic Earth structures in tomographic inversions that use earthquakes as sources.

Acknowledgments

References

Amorese, D., J. L. Lagarde, and E. Laville (1999). A point pattern analysis of the distribution of earthquakes in Normandy (France), *Bull. Seism. Soc. Am.* **89,** 742–749.

Aster, R., P. Shearer, and J. Berger (1990). Quantitative measurements of shear-wave polarizations at the Anza network, Southern California, *J. Geophys. Res.* **95,** 12449–12474.

Block, L. V., C. H. Cheng, M. C. Fehler, and W. S. Phillips (1994). Seismic imaging using microearthquakes induced by hydraulic fracturing, *Geophysics* **59,** 102–112.

Dodge, D. A., G. Beroza, and W. Ellsworth (1996). Detailed observations of California foreshock sequences: implications for earthquake initiation processes, *J. Geophys. Res.* **101,** 22371–22392.

Fehler, M., L. House, and H. Kaieda (1987). Determining planes along which earthquakes occur: method and application to earthquakes accompanying hydraulic fracturing, *J. Geophys. Res.* **92,** 9407–9414.

Fehler, M. (1989). Stress control of seismicity patterns observed during hydraulic fracturing experiments at the Fenton Hill hot dry rock geothermal energy site, New Mexico, *Int J. Rock Mech. Min. Sci. & Geomech. Abstr.* **26,** 211–219.

Fehler, M., and P. Johnson (1989). Determination of fault planes at Coalinga, California by analysis of patterns in aftershock locations, *J. Geophys. Res.* **94,** 7496–7507.

Fehler, M. (1990). Identifying the plane of slip for a fault plane solution from clustering of locations of nearby earthquakes, *Geophys. Res. Lett.* **17,** 969–972.

Fehler, M. L. House, W. S. Phillips, and R. Potter (1998). A method to allow temporal variation of velocity in travel-time tomography using microearthquakes induced during hydraulic fracturing, *Tectonophysics* **289,** 189–202.

Fremont, M.-J., and S. D. Malone (1987). High precision relative locations of earthquakes at Mount St. Helens, Washington, *J. Geophys. Res.* **92,** 10223–10236.

Gillard, D., A. M. Rubin, and P. Okubo (1996). Highly concentrated seismicity caused by deformation of Kilauea's deep magma system, *Nature* **384,** 343–346.

Haase, J., P. Shearer, and R. Aster (1995). Constraints on temporal variations in velocities near Anza, California from analysis of similar event pairs, *Bull. Seism. Soc. Am.* **85,** 194–206.

House, L. (1987). Locating microearthquakes induced by hydraulic injections in crystalline rock, *Geophys. Res. Lett.* 919–921.

Ito, A. (1985). High resolution relative hypocenters of similar earthquakes by cross-spectral analysis method, *J. Phys. Earth* **33,** 279–294.

Jones, R., and R. C. Stewart (1997). A method for determining significant structures in a cloud of earthquakes, *J. Geophys. Res.* **102,** 8245–8254.

Menke, W. (1984). *Geophysical Data Analysis: Discrete Inverse Theory,* Academic Press, Orlando, Florida.

Michelini, A., and B. Bolt (1986). Application of the principal parameters method to the 1983 Coalinga, California aftershock sequence, *Bull. Seism. Soc. Am.* **76,** 409–420.

Moriya, H., K. Nagano, and H. Niitsuma (1994). Precise Source Location of AE Doublets by Spectral Matrix Analysis of Triaxial Hodogram, *Geophysics* **59,** 36–45.

Nadeau, R., W. Foxall, and T. McEvilly (1995). Clustering and periodic recurrence of microearthquakes on the San Andreas fault at Parkfield, California, *Science* **267,** 503–507.

Phillips, W. S., L. House, and M. Fehler (1997). Detailed joint structure in a geothermal reservoir from studies of induced microearthquake clusters, *J. Geophys. Res.* **102,** 11745–11763.

Poupinet, G., W. L. Ellsworth, and J. Frechet (1984). Monitoring velocity variations in the crust using earthquake doublets: an application to the Calivaras Fault, California, *J. Geophys. Res.* **89,** 5719–5731.

Rubin, A., D. Gillard, and J.-L. Got (1999). Streaks of microearthquakes along creeping faults, *Nature* **400,** 635–641.

Shearer, P. (1997). Improving local earthquake locations using the L1 norm and waveform cross-correlation application to the Whittier Narrows, California aftershock sequence, *J. Geophys. Res.* **102,** 8269–8293.

Shearer, P. (1998). Evidence from a cluster of small earthquakes for a fault at 18 km depth beneath Oak Ridge, Southern California, *Bull Seism. Soc. Am.* **88,** 1327–1336.

Los Alamos Seismic Research Center
Los Alamos National Laboratory
Los Alamos, NM 87545
  (M. F., W. S. P., L. H.)

ABB Offshore Systems
Penryn, Cornwall, U.K.
  (R. H. J.)

Department of Earth and Environmental Science and Research Center
New Mexico Tech
Socorro, NM 87801
  (R. A., C. R.)